Applied Thermal Engineering 202 (2022) 117827

Contents lists available at ScienceDirect

Applied Thermal Engineering

journal homepage: www.elsevier.com/locate/apthermeng

Experimental study of water freezing process improvement using ultrasound

Hooman Daghooghi-Mobarakeh, Varun Subramanian, Patrick E. Phelan *

School for Engineering of Matter, Transport & Energy, Arizona State University, Tempe, AZ 85287-6106, USA

ARTICLE INFO

Keywords:
Ultrasound
Supercooling
Phase change
Freezing
Water
Energy efficiency

ABSTRACT

The phase change process of freezing water is an important application in several fields such as ice making, food freezing technologies, pharmaceuticals, etc. Due to the widespread usage of ice-related products, process improvements in this technology can potentially lead to substantial energy savings. It is well known that supercooling has a negative effect on the overall time and energy consumption of the freezing process. Therefore, ultrasound is proposed as a technique to improve the freezing process by eliminating the supercooling effect and the resulting energy savings is investigated. An experimental study was conducted to analyze the energy expenditures in the freezing process with and without the application of ultrasound. After a set of preliminary experiments, an intermittent application of ultrasound at 3.52 W & 8.25 W power levels was found to be more effective than constant-power application. The supercooling phenomenon was thoroughly studied through iterative experiments. It was also found that the application of ultrasound during the freezing process led to the formation of shard-like ice crystals. From the intermittent ultrasound experiments performed at 3.52 W & 8.25 W power levels, energy savings relative to no-ultrasound processes of 12.4% and 10.8% were observed, respectively.

1. Introduction

The process of freezing water is an important application in a variety of fields such as ice making, food freezing technologies, pharmaceuticals, ice slurry cold storage, etc. [1]. A study conducted by the US Department of Energy in 2009 estimated that a total of 1.23 Quads/yr of primary energy was used in commercial refrigeration equipment under which ice machines exclusively accounted for 0.28 Quads/yr of primary energy [2]. Fisher et al. conducted an independent study and suggested that the total inventory of ice machines in the USA was between 2.5 and 3 million units [3]. Yashar et al. investigated the energy consumption of automatic ice makers installed in domestic refrigerators and found that the range of tested products consumed between 0.249 and 0.652 kWh per kilogram of ice, which caused approximately 12−20% of additional energy consumption in an individual refrigerator [4]. Therefore, it can be observed that there are considerable energy savings potential in this area. The freezing process of water has been extensively investigated, and a phenomenon known as supercooling was found to occur which had a negative impact on the phase change process [5–7]. Supercooling (or undercooling) is the process of decreasing the temperature of a fluid below its melting/freezing point while it remains in a liquid state. This occurs when there is an absence of a seed crystal or nucleus which can initiate the formation of a crystal structure [8].

Dorsey reported that water can be supercooled until −20 °C using ordinary freezing methods and explored various parameters that can influence the supercooling of water such as preheating, filtration, duration of cooling, rate of nucleation, volume of water and mechanical initiation of freezing [9].

Ultrasound has long been used to intensify various processes, which have been mainly attributed to three major mechanisms: acoustic cavitation, acoustic streaming and oscillating pressure [10–14]. Ultrasound was used by several researchers as a potential method to overcome supercooling and improve the heat transfer in the freezing process of water to ice [1,15–21]. Inada et al. reported that when ultrasonic vibration was applied at 28 kHz and for power levels from 0 to 100 W, freezing was successfully initiated in both tap water and pure water. This was attributed to the ultrasonic cavitation phenomenon which helped create nucleation sites [1]. Zhang et al. utilized ultrasound at 39 kHz and 0.44 W/cm^2 intensity to further investigate the generation of ice slurries from supercooled water as well as the effect of bubble nuclei. It was reported that a high density of fine ice crystals was observed at the onset

* Corresponding author.
E-mail address: phelan@asu.edu (P.E. Phelan).

https://doi.org/10.1016/j.applthermaleng.2021.117827
Received 8 July 2021; Received in revised form 14 November 2021; Accepted 17 November 2021
Available online 26 November 2021

Nomenclature

ρ_c	coolant density kg m^{-3}
θ	phase angle rad
δt	time increment s
Δt	time period s
ΔT_C	coolant inlet & outlet temperature difference °C
ω	angular frequency Rad^{-1}
σ	surface tension N m^{-1}
μ	dynamic viscosity Pa s
COP	coefficient of performance -
c_p	specific heat J kg^{-1} K^{-1}
E_C	cooling energy J
E_T	total energy J
E_T	total energy J
$E_{T,NUS}$	total energy without ultrasound J
$E_{T,US}$	total energy under ultrasonication J
E_{US}	ultrasonic energy J
I_{rms}	root mean square current A
Nu_{Cyl}	Nusselt number -
Nu_H	Nusselt number -
Nu_V	Nusselt number -
P_a	acoustic pressure Pa
P_C	cooling power W
Pr	Prandtl number -
Ra_D	Rayleigh number -
Ra_L	Rayleigh number -
R_{max}	bubble radius upon implosion μm
P_{US}	ultrasonic power W
T	temperature °C
TC	thermocouple -
T_{Nuc}	nucleation temperature °C
UE	ultrasonic enhancement -
$\dot{V}$	feed water flow rate ml min^{-1}
V_{rms}	root mean square voltage V

Table 1
Summary of previous work on ultrasound-induced enhancements in water freezing processes.

REF	Frequency (kHz)	Ultrasonic Intensity (W/cm^2)	Observations
[1]	28	0–0.65	Reported that ultrasonic vibration induces phase change of supercooled water and proposed it as method to actively control the freezing temperature of supercooled water.
[17]	39	0.44	Observed the generation of ice slurries from supercooled water using ultrasound and established that the number of cavitation bubble sites increases phase change probability.
[18]	45	0.13 & 0.26	It was reported that higher levels of ultrasonic intensity showed better performance in terms of inducing phase change into ice.
[19]	39	0.44	A higher probability of ice nucleation within 0.5–1.1 s after the onset of ultrasonic irradiation was observed in water supersaturated with air bubbles.
[20]	20	–	Studied the effect of primary and secondary pulsed ultrasonication and reported that the secondary pulse led to the fragmentation of the formed ice crystals caused by the cavitation bubbles.
[23]	20	0.14–1.27	Results showed that the supercooling degree was reduced with the combined application of ultrasound and nanoparticles.

of ultrasound and the effect of ultrasound improves with an increase in the number of bubble nuclei sites [17]. Hozumi et al. reported that ultrasound applied at 45 kHz with an intensity of 0.13 W/cm^2 & 0.26 W/cm^2 helped in initiating nucleation. It was also reported that the nucleation effect increased with ultrasonic power and that the cavitation phenomenon was absent with reduced power [18]. Chow et al. studied the effect of a primary and secondary pulse of ultrasound at 20 kHz on supercooled water. The effect of the primary pulse reaffirmed the previous observation about increased ultrasonic power providing greater nucleation effects. It was reported that the effect of the secondary pulse led to fragmentation of pre-formed ice crystals and that there were flow patterns observed around cavitation bubbles which could have also contributed to the fragmentation [20].

The ultrasound-induced enhancements in freezing processes reported in previous studies are summarized in Table 1. Water is used as a thermal latent energy storage medium in several disciplines and has been evaluated as a phase change material (PCM), wherein supercooling was found to be undesirable [19,20]. Cui et al. and Jia et al. studied the combined effect of nanoparticles and ultrasound on the supercooling of water and found that the supercooling degree decreases with an increase in ultrasonic intensity and nanoparticle concentration [22,23]. Liu et al. investigated the effects of graphene oxide nanosheets and ultrasound on the supercooling and nucleation behavior of nanofluid PCMs and reported similar results in reducing nucleation time of the phase change process [24]. Many studies have been done regarding the effect of ultrasound during food freezing processes wherein various food types were analyzed and discussed in terms of freezing behavior under ultrasonic application [25–28]. It was established that ultrasound helps in increasing the freezing rate of the products and controlling the size and distribution of ice crystals [29]. It was also reported that the effects of ultrasound on the freezing processes were attributed to cavitation and microstreaming phenomena which helped in the nucleation and heat transfer enhancement, respectively [30]. The present study attempts to provide additional understanding of the effect that supercooling has on the freezing process of water and subsequently tests the application of ultrasound to overcome supercooling. Although past research has provided useful insights on the ultrasound-induced microscale phenomena related to freezing processes, the corresponding energy expenditures have not been clearly analyzed.

Given that the application of ultrasound is an energy-intensive process, and that ultrasonic energy is heat dissipating in nature, the application of ultrasound needs to be optimized when conducting experiments to ensure additional energy is not wasted and more so does not negatively affect the freezing process. An important aspect of using ultrasound to intensify any process is the energy consumption of the ultrasound device itself. Although the enhancement of the freezing process through elimination of supercooling by ultrasound has previously been verified, the feasibility of this method in terms of energy savings has not been analyzed quantitively and the energy consumption associated with the application of ultrasound relative to the potential energy savings either through elimination of supercooling or speeding up the process induced by ultrasound is still unclear [1,17–20,23]. In summary, this study seeks to establish the extent of supercooling overcome by ultrasound, analyze the effects of ultrasonic power level, and quantify the overall energy savings achieved using ultrasound in the phase change freezing process.

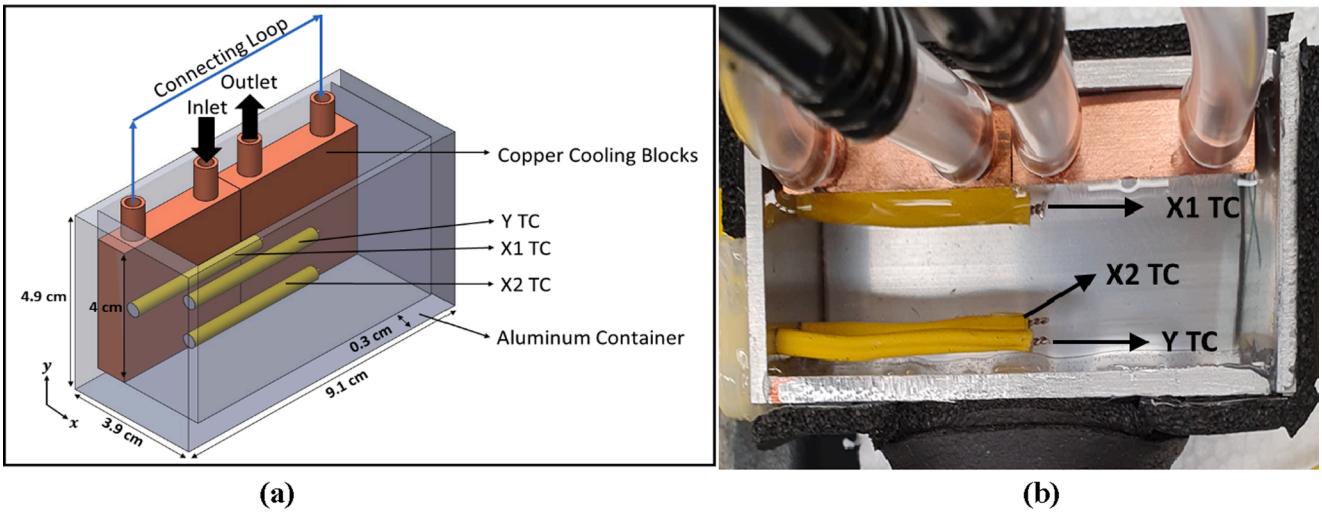

Fig. 1. Experimental schematic (a) and photo of the cooling module (b) (TC = thermocouple).

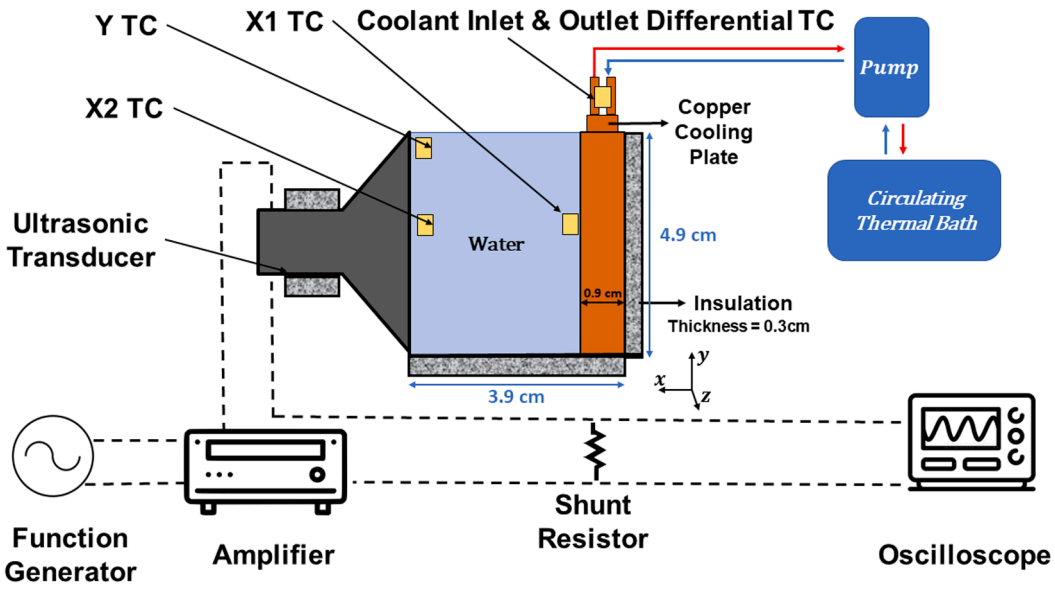

Fig. 2. Schematic diagram of the experimental set-up.

2. Materials and methodology

2.1. Cooling module specifications

Fig. 1 shows the schematic diagram of the cooling module that was utilized in the experiment. The cooling module consists of the aluminum container, copper cooling blocks and thermocouples. The material used for the container is aluminum 6061 alloy.

The outer dimensions of the cooling block are 4 cm × 4 cm × 0.9 cm. Three K-Type thermocouples (Omega Engineering-AWG 20) are placed inside the aluminum container at specific locations. These three thermocouples are utilized to properly capture the temperature variations across the cooling container during the freezing process.

The X2 thermocouple (reference) is placed on the opposite side of the copper cooling blocks and has a length of 2.45 cm, positioned at a height of 4.25 cm and 0.3 cm away from the wall opposite to the copper blocks.

The X1 thermocouple is placed close to the surface of the cooling blocks to monitor their surface temperature. The X2 thermocouple is placed at the same height as the X1 thermocouple but farthest from the cooling blocks and closest to the ultrasonic transducer. The Y thermocouple is placed 1.2 cm above the X1 thermocouple to measure the vertical temperature variations. A volume of 70 ml of tap water (TDS = 350 ± 7 ppm) is used to test the freezing process inside the cooling module. Tap water is used rather than distilled or purified water to accurately replicate water freezing applications in residential, commercial, and industrial applications. The top surface is covered with a 0.5- cm-thick layer of styrofoam thermal insulation material after the water is poured in during the experiment.

2.2. Experimental procedure

The schematic diagram of the experiment is shown in Fig. 2. The main components of the experimental set-up are the cooling module (Fig. 1), a 28 kHz-rated ultrasonic transducer, a function generator (Siglent Technologies SDG1032X), a high frequency-low slew rate amplifier (AALABSYSTEMS A-303), a power supply (PROTEK P6000), a pump and circulating thermal bath (Cole-Parmer Polystat). A 50% solution of ethylene glycol and water is used as the heat transfer fluid inside the thermal bath.

Taking the operating temperature of the pump into consideration, a

coolant temperature of −10 °C was chosen. Throughout the experiments, the temperature of the coolant varied ± 0.9 °C. Therefore, density ($\rho_c = 1085.4 \mathrm{kgm}^{-3}$) and specific heat ($C_p = 3.166 \mathrm{kJkg}^{-1}\mathrm{K}^{-1}$) of 50% diluted ethylene glycol solution at −10 °C were used for subsequent calculations [31].

The coolant inlet and outlet temperature difference was measured using a K-type differential thermocouple (Omega Engineering-AWG 20) which was used to calculate the supplied energy into the system.

All the thermocouples were calibrated using a Thomas Scientific reference thermometer which is certified as per NIST standards (certification number: 4244–11552989). All thermocouples were ascribed with an accuracy of ± 0.05 °C. The feed water flow rate was measured and controlled at 237 ml/min using a turbine flowmeter (Omega Engineering-FLR1008). An extra thermocouple was placed at the outer surface of the insulation material to measure the insulation heat gains. To operate the ultrasonic transducer at maximum efficiency, the resonant frequency of the transducer/container assembly was determined. The ultrasonic transducer and the shunt resistor were connected in series and using three voltage probes to measure the voltage differences across the transducer and shunt resistor, the impedance of the fully loaded transducer/container assembly under operating conditions was determined. The resonant frequency of the unloaded transducer provided by the supplier, 28 kHz (APC 90–4040) was validated, and the resonant frequency of the water-filled transducer/container assembly was measured to be 26.8 kHz. The temperature measurements were taken using a NATIONAL INSTRUMENTS data acquisition module (NI 9212) every 1 s. The experiments were conducted as *non-ultrasonic* and *ultrasonic* freezing processes. In the latter type of experiments, the ultrasonication was applied immediately after the first thermocouple temperature readings reached 0 °C and concluded once the last thermocouple reading dipped below 0 °C. This procedure was devised to ensure that ultrasound was only applied during the water phase change process during which the temperature of the water remained at 0 °C. The overall freezing process was continued until all the temperature readings reached −2 °C. The instantaneous input cooling power P_C supplied for each experiment was calculated as the following:

$$P_C = \rho \dot{V} C_p \Delta T_C \tag{1}$$

where ρ is the density of the coolant, $\dot{V}$ the coolant flow rate, C_p the specific heat capacity of the coolant and ΔT_C the temperature difference between the inlet and outlet temperatures of the coolant upon entering and leaving the cooling blocks, respectively. The power supplied to the ultrasonic transducer was also accounted for in the ultrasonic freezing process as

$$P_{US} = V_{rms} I_{rms} cos\theta \tag{2}$$

where $V_{rms}$is the root mean square value of voltage across the transducer, $I_{rms}$the root mean

square value of alternating current passing through the transducer, and θ the phase angle between the voltage and current. For the ultrasonic freezing experiments, the amplifier is fed with peak-to-peak voltage signals of 10 $V_{p\text{-}p}$ and 20 $V_{p\text{-}p}$ which depending on transducer impedance at the resonant frequency resulted in 3.52 W and 8.25 W ultrasonic power levels respectively. The total energy consumed to freeze the sample consists of the cooling energy transferred by the coolant through the cooling blocks and the ultrasonic energy delivered by the ultrasonic transducer:

$$E_T = E_C + E_{US} = \frac{1}{COP}\sum P_C(i)\delta t + P_{US}\Delta t \tag{3}$$

where E_T is the total energy, E_C the cooling energy, E_{US} the ultrasonic energy, *COP* the refrigeration coefficient of performance,δt the time increment of measurement at which cooling power input is evaluated, and Δt the total time period of ultrasonication. A *COP* of 1.8 is adopted to approximate real-world refrigeration [4]. The ultrasonic enhancement *UE* indicates the feasibility of integrating ultrasound in a freezing process from an energy-saving point of view and can be written as:

$$UE = \frac{E_{T,NUS} - E_{T,US}}{E_{T,NUS}} \tag{4}$$

where $E_{T,NUS}$ is the energy consumption for a non-ultrasonic freezing process (i.e., conventional freezing) and $E_{T,US}$ the energy consumption for an ultrasound-assisted freezing processes.

Table 2
Uncertainties of measured parameters.

Parameters	Uncertainty	Unit
$\dot{\mathbf{V}}$	±3%	kg s^{-1}
$\mathbf{\Delta T_C}$	±0.05	°C
V_{rms}	±0.2%	V
I_{rms}	±0.2%	A

2.3. Uncertainty analysis

The general calculation for the bias uncertainty (U_y) in a given experimental result *y* can be stated as [32]:

$$U_y = \sqrt{\left(\frac{\partial y}{\partial x_1}U_{x_1}\right)^2 + \left(\frac{\partial y}{\partial x_2}U_{x_2}\right)^2 + \left(\frac{\partial y}{\partial x_3}U_{x_3}\right)^2 + \cdots + \left(\frac{\partial y}{\partial x_n}U_{x_n}\right)^2} \tag{5}$$

where Ux_1, Ux_2, Ux_3 … U_{xn} are the uncertainties in the primary measurements. The accuracies of the various primary measurements are given in Table 2. For one such case, the bias uncertainty $U_{E_{bias}}$ associated with the cooling energy input E_C is obtained using:

$$U_{E_{bias}} = \sqrt{\left(\frac{\partial E}{\partial \dot{m}}U_{\dot{m}}\right)^2 + \left(\frac{\partial E}{\partial \Delta T_C}U_{\Delta T_C}\right)^2} \tag{6}$$

The total uncertainties including precision uncertainties associated with the results are discussed in Section 3.3.

2.4. Heat gain

In order to limit heat gain from the external environment, all exposed surfaces of the cooling module were fully insulated. Although adequate insulation was applied, it is important to measure the amount of heat gain in order to accurately interpret the experimental results. The outer surface temperature of the insulation was recorded over the course of the experiments to calculate the heat gain during the overall duration of the freezing process. The average recorded insulation temperature was utilized to calculate the heat flux entering the system. The cooling module container surfaces were treated as horizontal and vertical surfaces, while the ultrasonic transducer attached to the side of the container was treated as a horizontal cylinder. Assuming natural convection heat transfer and the air properties at the film temperature $T_f = 19^{\circ}$C, the Nusselt numbers for the horizontal sides, Nu_H, and the vertical sides, Nu_V, of the cooling module and the transducer, Nu_{Cyl}, respectively are determined using [33]:

$$Nu_H = 0.27 {Ra_L}^{1/4} \tag{7}$$

$$Nu_V = \left\{0.825 + \frac{0.387 {Ra_L}^{1/6}}{\left[1 + (0.492/Pr)^{9/16}\right]^{8/27}}\right\}^2 \tag{8}$$

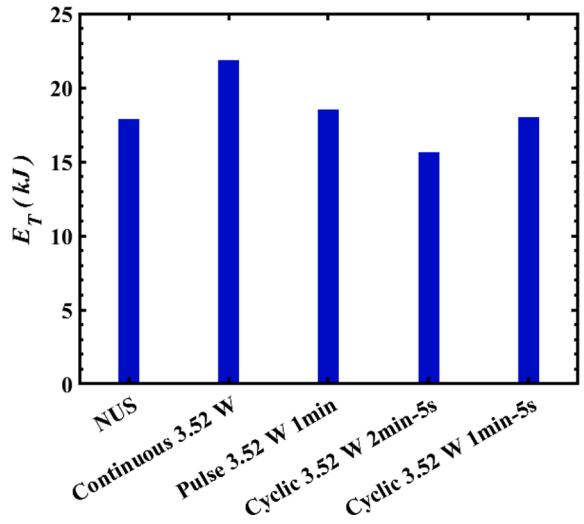

Fig. 3. The total energy consumption of various ultrasonicated freezing experiments.

$$Nu_{Cyl} = \left\{ 0.6 + \frac{0.387 Ra_D{}^{1/6}}{\left[1 + \left(\frac{0.559}{Pr}\right)^{9/16}\right]^{8/27}} \right\}^2 \tag{9}$$

where Ra_L is the Rayleigh number based on the length of the vertical and horizontal sides, Ra_D the Rayleigh number based on the diameter of the transducer and Pr the Prandtl number. The total average heat gain for the duration of the experiment was calculated to be 0.6 W which corresponds to 6% of the average supplied cooling power.

2.5. Input power proportionality

The cooling module dimensions were designed by taking into consideration the transducer contact area and the cooling energy input into the system. As this set of experiments constitute a comparative study to evaluate the energy saving potential with and without the application of ultrasound, the cooling module size is not particularly significant in the comparative analysis.

Nevertheless, to ensure the practical applicability of the experiment, the ultrasonic power levels are applied proportional to the module size. As stated earlier, a study reported that the energy consumption in domestic refrigerators consumed between 0.249 and 0.652 kWh per kilogram of ice [4], which is comparable to the average cooling energy of 0.36 kWh per kilogram of ice applied in this study. The cyclic 3.52 W and 8.25 W ultrasonic input powers applied during the phase change process correspond to total ultrasonic energies of 197 J and 462 J, or 1.1% and 2.6% of the average total cooling energy of 17800 J, respectively.

The ultrasonic intensities of 0.08 W/cm^2 and 0.18 W/cm^2 corresponding to 3.52 W and 8.25 W ultrasonic power, respectively, used in this study were deliberately kept low to maintain a sense of feasibility for the scaling-up of the geometry for industrial application.

3. Results and discussion

A set of preliminary non-ultrasound (NUS) and ultrasound-assisted (US) freezing experiments was performed to observe the supercooling effect in water and properly understand the appropriate application of ultrasound to improve this process. Different types of ultrasound-assisted freezing processes such as *continuous ultrasonic*, *pulsed ultrasonic*, and *cyclic ultrasonic* were performed. A *continuous ultrasonic freezing process* refers to constant sonication during the freezing process which is inherently inefficient due to excess energy consumption and heat dissipation of the acoustic energy. A *pulsed ultrasonic freezing process* is the one-time application of ultrasound which is used to initiate the nucleation of ice at the beginning stages of supercooling when the water temperature first dips below 0 °C. *Cyclic ultrasonic freezing experiments* are optimized tests wherein ultrasound is applied for a short time period and repeated at given intervals to maintain the ultrasonic effect over the course of the entire freezing process for a low overall energy consumption. The total energy consumption of various ultrasonicated freezing experiments are presented in Fig. 3.

As can be inferred from Fig. 3, amongst various preliminary ultrasound-assisted freezing experiments, the cyclic 5-second-long pulses repeated every 2 min demonstrated lower energy consumption rates when compared with the other ultrasonicated freezing experiments. Therefore, further experiments were focused on these conditions to obtain greater energy enhancements.

3.1. Non-ultrasonic freezing process

Since the non-ultrasound freezing processes are considered as baseline experiments in terms of energy consumption, it is important to properly understand the underlying phenomena occurring in the process. Fig. 4 (a) showcases the temperature variations of water measured

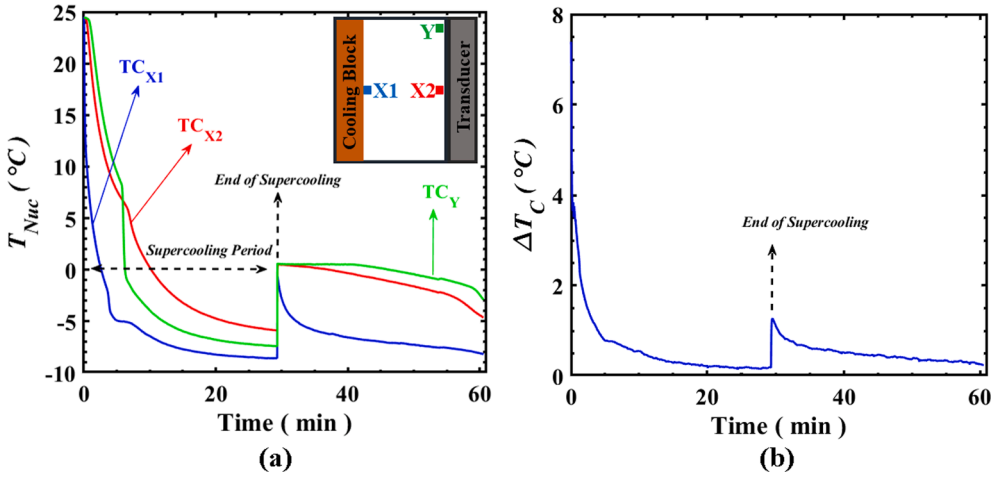

Fig. 4. Temperature variation across the container with super cooling indication (a) and coolant inlet & outlet temperature difference (b) in a non-ultrasonic freezing process.

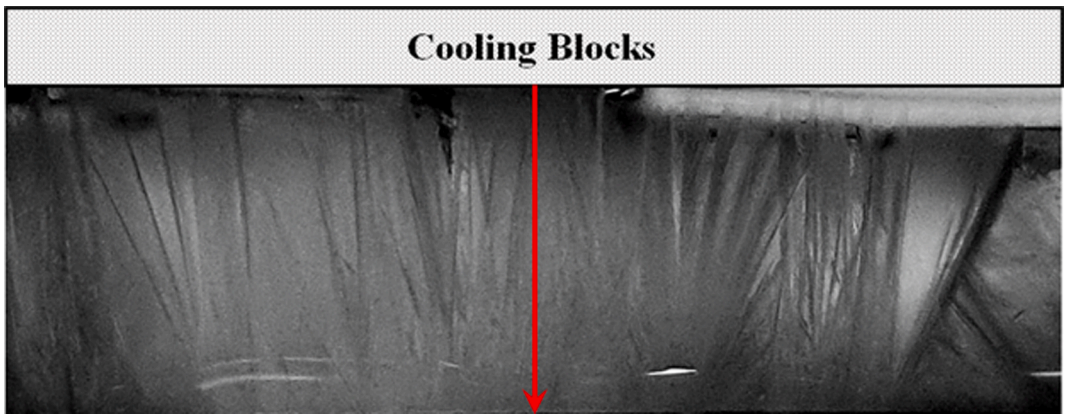

Fig. 5. Formation of an ice/water slurry at the end of the supercooling period in a non-ultrasonic freezing process (top view).

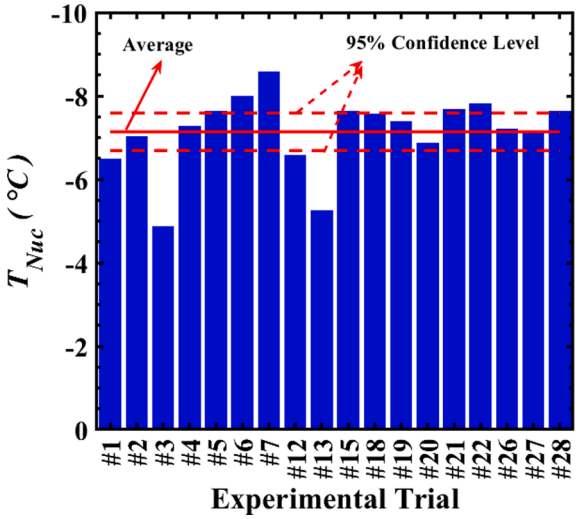

Fig. 6. Nucleation temperatures (supercooling degree), T_{Nuc}, of all non-ultrasonic freezing experiments.

at three locations during the non-ultrasound experiment. It can be observed that the temperature measured at the X1 thermocouple location (positioned low and close to the cooling surface) starts to dip below 0 °C around 2.6 min into the experiment which signifies the start of supercooling. During the supercooling period, the undisturbed water remains stagnant and in a liquid state even as the temperatures continue to decrease to sub-zero levels. At a certain temperature threshold around −8.6 °C at approximately the 29th minute, an instantaneous freezing phenomenon occurs which results in a sudden jump in the temperatures to just above 0 °C. The freezing phenomenon results in the formation of ice slurries or an ice-water mixture which cannot be classified as a complete solid or liquid structure as the formed ice crystals are unstable and quickly melt back into water. Interestingly, in all non-ultrasonic freezing processes, the crystalline lines of the slurry mainly form in the direction perpendicular to the cooling blocks as shown in Fig. 5. After this point, the freezing process continues at a steady rate with solid ice being formed from the side of the copper cooling blocks. The temperatures at the other thermocouples stagnate at 0 °C until the ice formation reaches the locations of the specific thermocouples which results in a temperature drop. For example, the X1 thermocouple temperature is the first to drop below 0 °C at the 30th minute as it is closest to the copper cooling blocks, and therefore experiences freezing earlier than the other thermocouples. The experiment is stopped when the last thermocouple drops to a temperature of −2 °C which is indicated by the Y thermocouple measured temperature in this particular case as shown in Fig. 4 (a).

The coolant inlet and outlet temperature differences, $\Delta T_{Cooling}$, are measured over the course of the experiment as shown in Fig. 4 (b). It can be observed that $\Delta T_{Cooling}$ steadily reduces during the supercooling period but there is a sudden rise in $\Delta T_{Cooling}$ corresponding to the instantaneous freezing phenomenon that occurs at the end point of the supercooling period. This increase in $\Delta T_{Cooling}$ can be attributed to the sudden temperature rise observed in Fig. 4 (a) and the latent heat energy absorbed by the water during the instantaneous freezing process. After the sudden peak in $\Delta T_{Cooling}$, the temperature differences again begin to reduce steadily. Previous studies reported the extent of supercooling of water to occur at a variety of temperatures [1,18,20]. Therefore, the non-ultrasound freezing experiment was repeated 18 times under the same conditions to properly understand the range of temperatures over which supercooling occurs.

Fig. 6 showcases the repeated non-ultrasound experimental trials and the supercooling degrees (ice nucleation temperatures) observed during supercooling for each trial. From Fig. 6, it is noticeable that for the consecutive nominally identical experiments that were conducted, there is substantial variability in the temperature of ice nucleation (-7.14 ± 0.45 °C) and this could be due to several reasons such as preheating, effect of filtration, effect of duration of cooling, rate of nucleation, and mechanical initiation of freezing [9]. To maintain a realistic approach in the freezing process, no cleaning of the cooling plates and the container was carried out.

3.2. Ultrasound-assisted freezing process

After establishing the supercooling effect in the freezing process of water and testing the preliminary ultrasonic experiments, the optimized cyclic P_{US} = 8.25 W and 3.52 W ultrasonic experiments were further investigated wherein ultrasound was applied every 2 min for a duration of 5 s [1]. Here, the ultrasound is applied when the water temperature first reaches 0 °C. The X1 thermocouple as shown in Fig. 7 (a) and (c) is the first thermocouple to reach 0 °C at around the 3rd minute of the experiment, at which point P_{US} = 8.25 W or 3.52 W of ultrasound is applied for a duration of 5 s. Immediately after ultrasound is first applied, a sudden temperature rise is observed in the X1 thermocouple location. This is attributed to the freezing process that produces ice at the surface of the cooling blocks and at the location of the X1thermocouple.

This indicates that freezing was successfully initiated using ultrasound and supercooling of water was avoided. After the formation of an initial solid layer of ice, supercooling does not occur at any other point inside the water domain as the solid ice layer acts as a nucleation seed point for the generation of further ice crystals [9]. Therefore, as the experiment continued, the temperature across the bed as indicated by the other thermocouples approached 0 °C but did not dip below 0 °C.

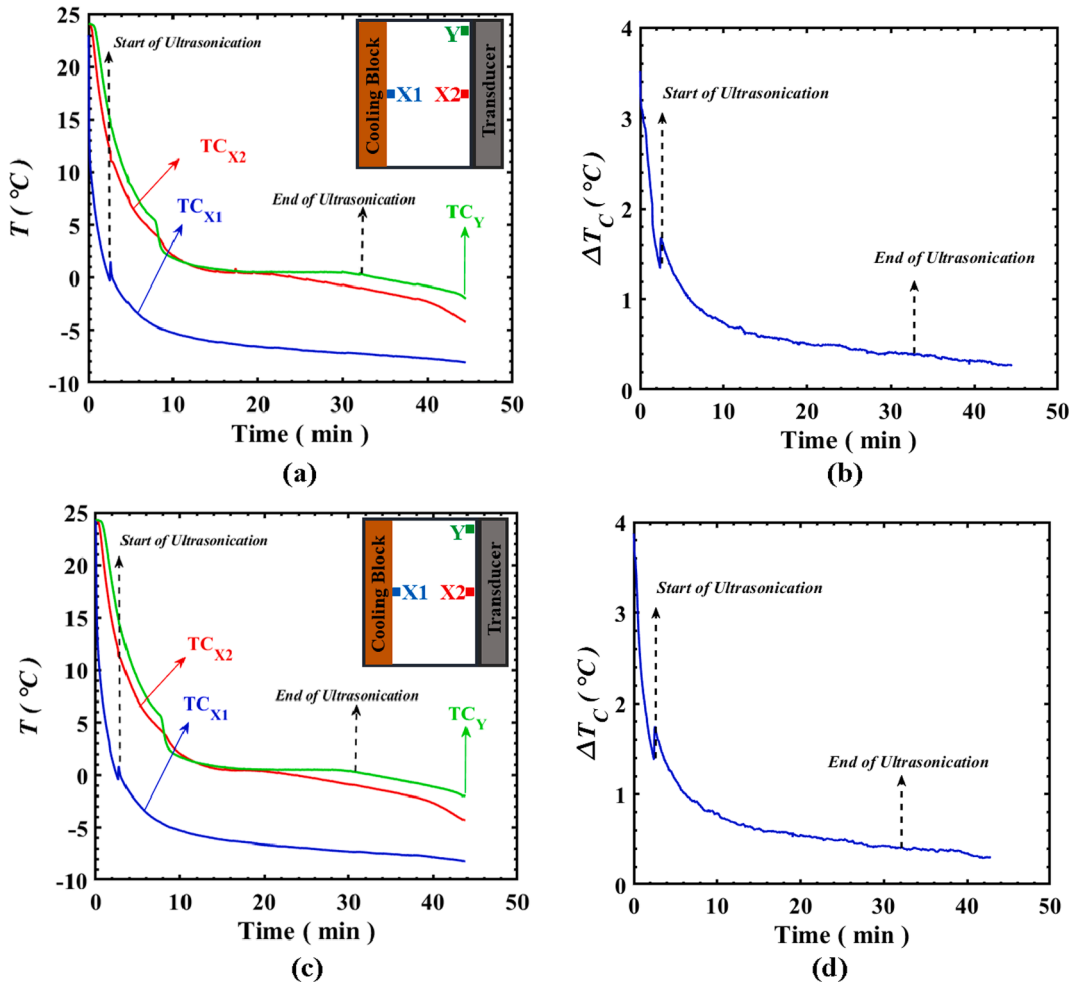

Fig. 7. Temperature variation across the container (a) in an 8.25 W and (c) in an 3.52 W ultrasound-assisted freezing process and coolant inlet & outlet temperature difference (b) in an 8.25 W and (d) in an 3.52 W ultrasound-assisted freezing process.

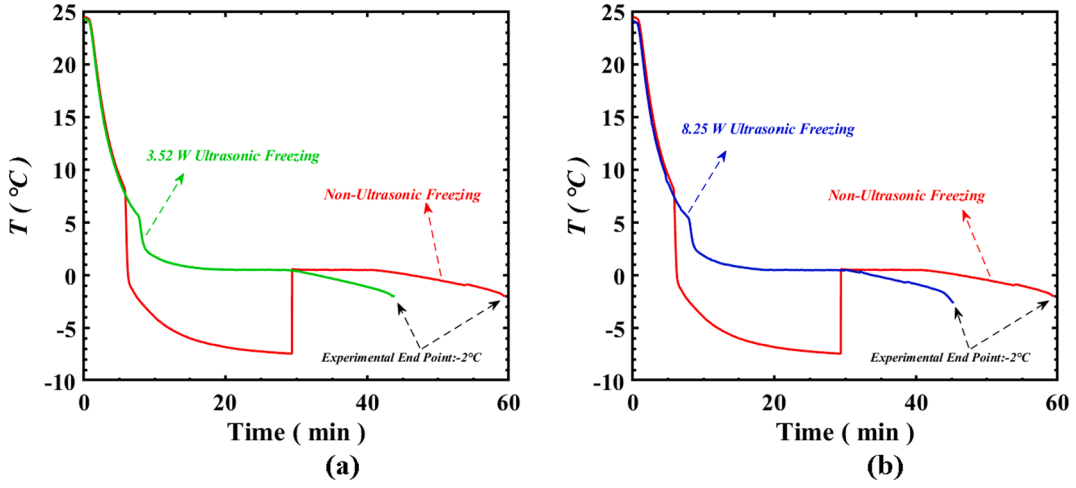

Fig. 8. Comparison of Y thermocouple measured temperature between P_{US} = 3.52 W cyclic (a), P_{US} = 8.25 W cyclic (b) and non-ultrasound freezing process.

Ultrasound was consistently applied for a duration of 5 s every 2 min until the last thermocouple measurement dropped below 0 °C, after which the application of ultrasound was stopped. Fig. 7 (b) and (d) show the temperature difference (ΔT_C) between the coolant inlet and outlet temperatures for the 3.52 W and 8.25 W cyclic ultrasonic experiments. As observed in Fig. 7 (b), the start of ultrasonication results in a sudden jump in ΔT_C which can be attributed to the freezing initiated by the ultrasonic waves. After an initial rise in $\Delta T_{Cooling}$, it steadily reduces over the course of the experiment. A similar graphical trend is observed in the temperature measurements for the 3.52 W cyclic ultrasound experiments which proves that ultrasound applied at 3.52 W also helps in initiating freezing and eliminating supercooling. The sudden rise in

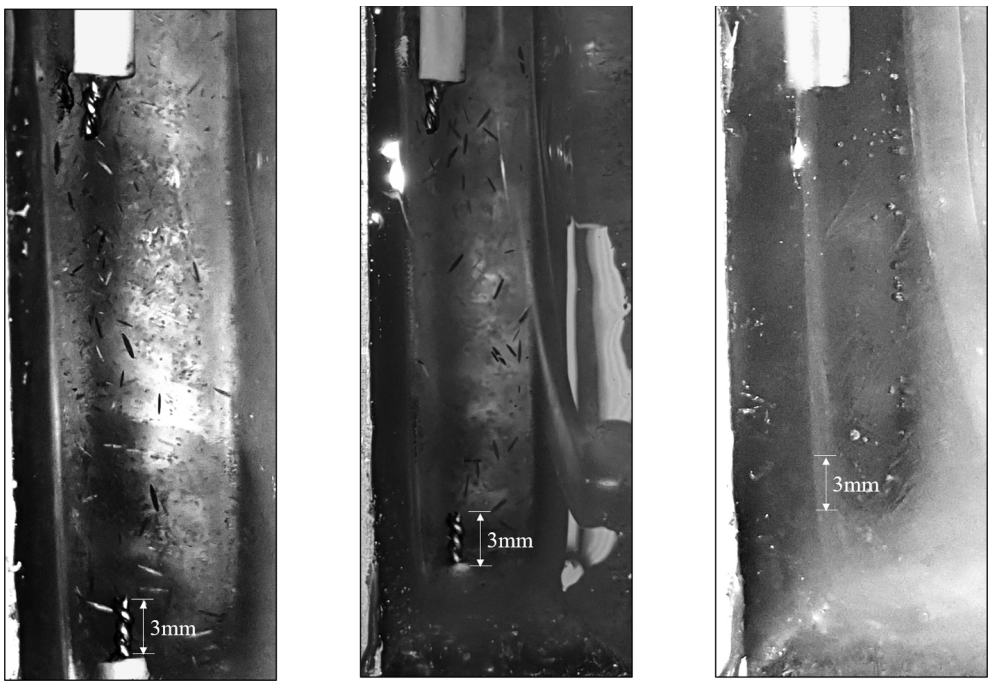

Fig. 9. Presence of ice crystals in the 8.25 W (left), 3.52 W (middle) cyclic ultrasonic freezing processes and the absence of crystals in the non-ultrasound freezing process (right).

Table 3
The average length of the ice shards and concentration in both ultrasonic freezing processes.

P_{US} (W)	Average length of ice shards (mm)	Average population of ice shards (shards/cm^2)
3.52	0.94	5
8.25	1.3	9

$\Delta T_{Cooling}$ which is observed in both ultrasonic and non-ultrasonic freezing processes caused by the release of the latent heat of fusion is directly proportional to the amount of ice formed. In the case of non-ultrasonic freezing, the formation of ice slurry throughout the container at the end of the supercooling period results in release of a higher amount of heat and thus a higher rise in $\Delta T_{Cooling}$ (Fig. 4 (b)) while in ultrasonic freezing, a thin layer of ice is formed upon ultrasonication resulting in a lower release of heat and consequently a lower jump in $\Delta T_{Cooling}$ (Fig. 7 (b) and (d)). Fig. 8 shows a comparison of the temperature measurements between the non-ultrasound and $P_{US} = 8.25$ W and 3.52 W cyclic freezing experiment at the Y thermocouple location (relatively far from the cooling blocks and higher than the X1 thermocouple). The extent of supercooling can be observed in Fig. 8 wherein the non-ultrasonic freezing experiment the temperature of the water sample drops down significantly to −7.4 °C before freezing occurs. Whereas in the ultrasound-assisted freezing experiment, due to the elimination of supercooling through ultrasound, the water in liquid form does not experience sub-zero temperatures as was observed in previous work [1,18,23].

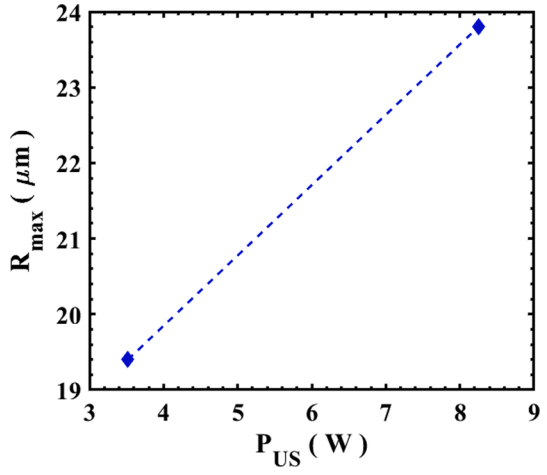

Fig. 10. The variation of the critical cavitation bubble radius in the ultrasonic freezing experiments.

There is a noticeable difference in the end points for the experiments which indicates that the cyclic ultrasound experiment significantly reduces the overall duration of the freezing process. This also contributes to the reduction in energy consumption for the ultrasonic experiments which is discussed later.

During the cyclic ultrasound-assisted freezing process, an unexpected phenomenon was observed. As the experiment proceeded, ice shards/crystals were found stagnating inside the water domain during the ultrasound-assisted freezing process. Fig. 9 shows the captured images of ice crystals/shards that were found in the 8.25 W and 3.52 W ultrasonic freezing processes which are compared with an image of a non–ultrasound freezing process taken at an equivalent time. It was also visually observed that the concentration and size of the crystals differed between the 8.25 W and 3.52 W ultrasonic freezing processes, wherein there was a greater concentration and size of ice crystals observed in the 8.25 W ultrasonic experiments. The average length of the ice shards and concentration in both ultrasonic freezing processes were obtained by analyzing 6 samples with *ImageJ* software and are provided in Table 3 [34].

Primarily in the ultrasonic experiments, sonication initiated the nucleation of ice which can be attributed to cavitation effects as reported by several others [1,17,35–37]. Although there is an agreement that acoustic cavitation is the responsible mechanism in the initiation of ice nucleation and eliminating supercooling, exactly how cavitation initiates nucleation remains a subject of controversy [36]. Hunt and Jackson suggested that following the significantly high positive pressure caused

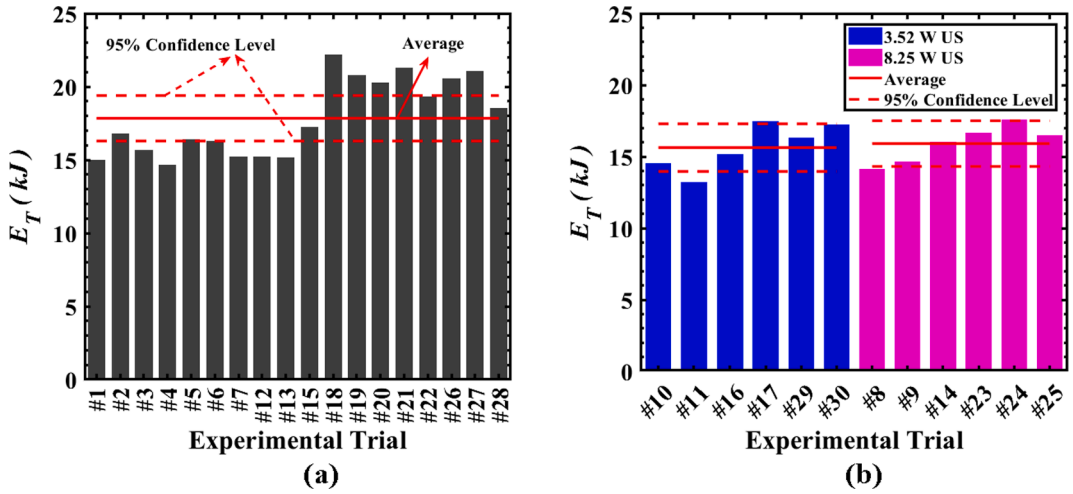

Fig. 11. Variation in total energy consumption of non-ultrasonic (a) and ultrasonic (b) freezing trials.

Table 4
The total uncertainty of $E_{T,NUS}$, $E_{T,US}$, and UE.

Parameter		Total uncertainty	unit
$E_{T,NUS}$		±8.7	%
$E_{T,US}$	3.52 W	±10.6	%
	8.25 W	±10.1	%
UE	3.52 W	±11.9	%
	8.25 W	±11.8	%

by the implosion of the cavitation bubble, a significantly high negative pressure establishes which in turn undercools the water initiating nucleation [36]. This explanation seems to be consistent with the size and concentration of ice shards/crystals observed in the present ultrasonic freezing experiments. The magnitude of the positive and consequently negative pressures following the implosion of a cavitation bubble is proportional to the critical radius of the cavitation bubble which is the bubble radius at the moment of the implosion; the larger the bubble is the more disruption it causes upon implosion and the higher the magnitude of alternating pressure [38,39]. The critical radius of a cavitation bubble R_{max} is determined from [40,41]:

$$\omega^2 \rho R_{max}^2 = 3\mu\left(P_a - \frac{2\sigma}{R_{max}}\right) \tag{10}$$

where ω is the ultrasound angular frequency ($\omega = 2\pi f$), μ the fluid kinematic viscosity, P_a the acoustic pressure, and σ the fluid surface tension.

The variation of R_{max} with P_{US} is shown in Fig. 10. The critical radius R_{max} and consequently the acoustic-cavitation-associated effects increase with an increase in P_{US}. At higher ultrasonic power $P_{US} = 8.25$ W the critical bubble radius is larger relative to that at $P_{US} = 3.52$ W resulting in larger and more concentrated ice shards.

3.3. Energy analysis

Although ultrasonication prevents supercooling, it comes at the potential expense of adding more energy to the system to generate ultrasound. So, the total energy consumption of the non-ultrasonic and ultrasound-assisted freezing processes needs to be compared and possible energy savings associated with application of ultrasound needs to be investigated. The total energy consumption E_T for all 18 non-ultrasonic, 6 low P_{US} (3.52 W) and 6 high P_{US} (8.25 W) freezing process trials corrected for refrigeration *COP* are shown in Fig. 11. To prevent any unintentional favoritism, the ultrasonic freezing process trials are randomly conducted in between the non-ultrasonic ones. It can be noticed from Fig. 11 that there is a relatively large variation in E_T. The precision uncertainty $U_{E_{prec}}$ associated with the total energy consumption is calculated using the Student's t-method [32].

The total uncertainty including the bias and precision (95% confi-

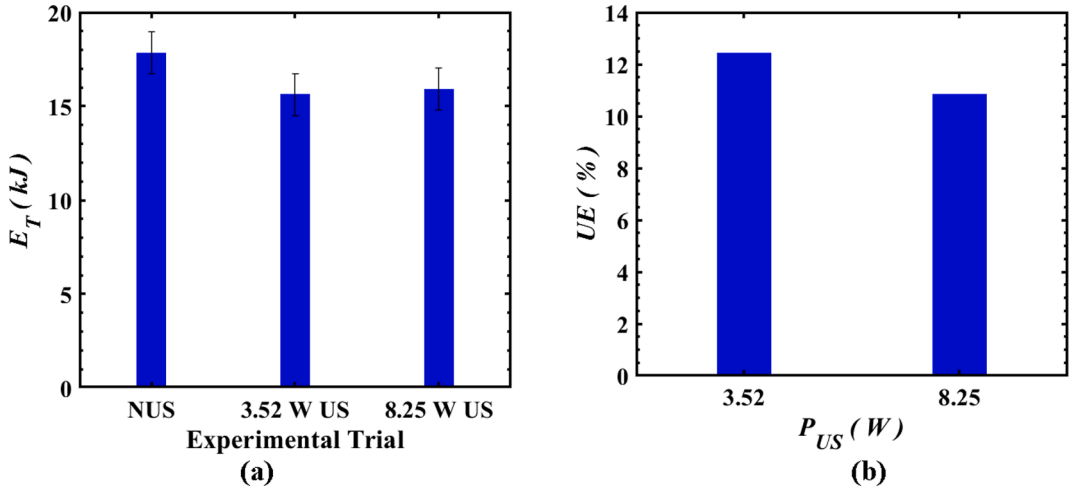

Fig. 12. The average total energy consumption (E_T) of the three freezing modes (a) and ultrasonic enhancement (UE) (b).

Table 5
The average overall freezing time of the non-ultrasonic, 3.52 W cyclic and 8.25 W cyclic ultrasonic-enhanced freezing processes.

P_{US} (W)	Average freezing time (s)	Time reduction (%)
0	2913	–
3.52	2651	9.9
8.25	2671	9.1

dence level) uncertainties for total energy without ultrasound $E_{T,NUS}$, total energy under ultrasonication $E_{T,US}$, and ultrasonic enhancement *UE* are provided in Table 4. There are a number of factors that potentially can affect the freezing process such as cooling rate, initial temperature, quality of water and mechanical vibration [9]. The cooling rate depends on the coolant inlet temperature, coolant flow rate and heat gain all of which are nominally held constant in this study.

The initial temperature of the water samples for all freezing processes is kept at 24 ± 0.5 °C and the same tap water sample (TDS = 350 ± 7 ppm) is stored and used for all freezing processes. One factor that could potentially cause the inconsistencies in both ultrasonic and non-ultrasonic freezing processes is the vibrational noise generated by the pump and the thermal bath. Vibrational noise even at low amplitudes could potentially initiate microscale nucleation of tiny ice crystals by means of cavitation if the frequency is low enough [41]. The average total energy consumption of the three freezing modes is shown in Fig. 12 (a). Theoretically speaking, the freezing process of this study including sensible cooling of water and ice and latent heat of freezing, which turns liquid water at 24 °C to ice at −4°C (final average temperature across the container) with consideration of the refrigeration coefficient of performance, requires 14 kJ of cooling energy which is in general agreement with the experimental results. It can be inferred from the figure that integration of ultrasound, regardless of ultrasonic power level, results in energy savings. At the higher ultrasonic input of P_{US} = 8.25 W the ultrasonic enhancement *UE* is 10.8% whereas at the lower ultrasonic input of P_{US} = 3.52 W the ultrasonic enhancement *UE* increases to 12.4%. This trend could be related to the acoustic dissipation which is an undesired byproduct of the ultrasonication which leads to heat generation that opposes the freezing process. The occurrence of supercooling in non-ultrasonic freezing processes results in an unnecessary sub-zero cooling of water in liquid form and consequently leads to an increase in energy consumption. Since the integration of ultrasound prevents supercooling, it results in lower energy consumption compared to non-ultrasonic freezing.

Additionally, the latent heat of solidification of water increases as the temperature decreases below 0 °C meaning that more energy is required to solidify water compared to the normal freezing process at 0 °C [42]. Another factor that differentiates the energy consumption of non-ultrasonic from ultrasound-assisted freezing processes is that by elimination of supercooling using ultrasound the freezing process occurs at a faster rate and the overall freezing period shortens by as much as 10%.

The average total freezing time of the non-ultrasonic, P_{US} = 3.52 W cyclic and 8.25 W cyclic freezing processes and their enhancement relative to the non-ultrasonic freezing process are presented in Table 5.

Interestingly, although integration of ultrasound saves time at both ultrasonic power levels, i.e. 8.25 W and 3.52 W, there is not much difference in the corresponding enhancements considering that the applied P_{US} varies by more than a factor of two.

4. Conclusion

The effect of ultrasound on the supercooling and freezing processes of water was investigated. The intensification of the freezing process by application of ultrasound with regard to overall duration of freezing and energy savings relative to added ultrasonic energy was analyzed. After a set of preliminary experiments, an optimized set of cyclic 5-second ultrasonic pulses every 2 min was found to be promising in terms of energy savings compared to a non-ultrasonic freezing process and was investigated in further detail. It was determined that the application of ultrasound at 3.52 W and 8.25 W power levels corresponding to 0.08 W/cm^2 and 0.18 W/cm^2 ultrasonic intensities, respectively, helped to eliminate supercooling and initiate ice nucleation.

Eighteen iterative runs of non-ultrasound freezing experiments were conducted to properly observe and measure the variable nature of the supercooling effect in water.

The application of ultrasound helped reduce the overall duration of the freezing process by ~ 10% which consequently reduced the overall energy consumption. It was also observed that the effect of ultrasonic waves during the freezing process resulted in the formation of ice crystals/shards of size and density proportional to ultrasonic power.

Due to the inherent vibrational noise of the experimental setup caused by the thermal bath and the pump which in turn affects the freezing process, there is a more-than-desired variation in the total energy consumption in both ultrasonic and non-ultrasonic freezing processes. The ultrasonic freezing trials were limited to 3.52 W and 8.25 W cyclic ultrasonication which resulted in an ultrasonic enhancement *UE* of 12.4 % ±11.9 % and 10.8 % ±11.8 %, respectively, compared to a non-ultrasonic-enhanced freezing process.

Declaration of Competing Interest

The authors declare that they have no known competing financial interests or personal relationships that could have appeared to influence the work reported in this paper.

Acknowledgment

This material is partially based upon work supported by the National Science Foundation, United States under Grant Number CBET – 1703670. Any opinions, findings, and conclusions or recommendations expressed in this material are those of the authors and do not necessarily reflect the views of the National Science Foundation.

References

[1] T. Inada, X. Zhang, A. Yabe, Y. Kozawa, Active control of phase change from supercooled water to ice by ultrasonic vibration 1. Control of freezing temperature, Int. J. Heat Mass Transf. 44 (23) (Dec. 2001) 4523–4531, https://doi.org/10.1016/S0017-9310(01)00057-6.

[2] "Energy Savings Potential and Research & Development Opportunities for Commercial Refrigeration," United States, Sep. 2009. https://doi.org/10.2172/1219982.

[3] D. Fisher, D. Cowen, A. Karas, F. Nickel, Commercial Ice Machines : The Potential for Energy Efficiency and Demand Response Types of Ice Machines Energy Efficiency and Performance of Ice Machines, ACEEE Summer Study Energy Effic. Build. 9–103 (2) (2012) 103–114.

[4] D. A. Yashar and K.-J. Park, "Energy Consumption of Automatic Ice Makers Installed in Domestic Refrigerators," *NIST Tech. Note 1697*, [Online]. Available: https://www.nist.gov/publications/energy-consumption-automatic-ice-makers-installed-domestic-refrigerators-nist-tn-1697.

[5] W. Cantrell, A. Kostinski, A. Szedlak, A. Johnson, Heat of freezing for supercooled water: Measurements at atmospheric pressure, J. Phys. Chem. A 115 (23) (2011) 5729–5734, https://doi.org/10.1021/jp103373u.

[6] Y. Liu, X. Li, P. Hu, G. Hu, Study on the supercooling degree and nucleation behavior of water-based graphene oxide nanofluids PCM, Int. J. Refrig. 50 (Feb. 2015) 80–86, https://doi.org/10.1016/j.ijrefrig.2014.10.019.

[7] K.-C. Tan, W. Ho, J.I. Katz, S.-J. Feng, A study of the occurrence of supercooling of water, Am. J. Phys. 84 (4) (2016) 293–300, https://doi.org/10.1119/1.4939792.

[8] P. Wilson (Ed.), Supercooling, InTech, 2012.

[9] N.E. Dorsey, The Freezing of Supercooled Water, Trans. Am. Philos. Soc. 38 (3) (Nov. 1948) 247, https://doi.org/10.2307/1005602.

[10] N. Gondrexon, Y. Rousselet, M. Legay, P. Boldo, S. Le Person, A. Bontemps, Intensification of heat transfer process: Improvement of shell-and-tube heat exchanger performances by means of ultrasound, Chem. Eng. Process. Process Intensif. 49 (9) (Aug. 2010) 936–942, https://doi.org/10.1016/j.cep.2010.06.007.

[11] M. Legay, O. Bulliard-Sauret, S. Ferrouillat, P. Boldo, N. Gondrexon, Methods to Evaluate Heat Transfer Enhancement in an Ultrasonic Heat Exchanger, Heat Transf. Eng. 41 (17) (2020) 1457–1472, https://doi.org/10.1080/01457632.2019.1649917.

[12] H. Daghooghi-mobarakeh, et al., Application of ultrasound in regeneration of silica gel for industrial gas drying processes, Dry. Technol. (2021) 1–9, https://doi.org/10.1080/07373937.2021.1929296.
[13] H. Daghooghi-Mobarakeh, et al., Ultrasound-assisted regeneration of zeolite/water adsorption pair, Ultrason. Sonochem. 64 (February) (Jun. 2020), https://doi.org/10.1016/j.ultsonch.2020.105042.
[14] H. Daghooghi Mobarakeh Bandara, K. Wang, L. Wang, R. Phelan, P.E. Miner, *et al.*, "Low-grade heat utilization through ultrasound-enhanced desorption of activated alumina/water for thermal energy storage," Aug. 2020, doi: 10.1115/POWER2020-16802.
[15] M. Dalvi-Isfahan, N. Hamdami, E. Xanthakis, A. Le-Bail, Review on the control of ice nucleation by ultrasound waves, electric and magnetic fields, J. Food Eng. 195 (Feb. 2017) 222–234, https://doi.org/10.1016/j.jfoodeng.2016.10.001.
[16] F. Baillon, F. Espitalier, C. Cogné, R. Peczalski, O. Louisnard, Crystallization and freezing processes assisted by power ultrasound, in: *Power Ultrasonics: Applications of High-Intensity Ultrasound*, Elsevier, 2015, pp. 845–874.
[17] X. Zhang, T. Inada, A. Yabe, S. Lu, Y. Kozawa, Active control of phase change from supercooled water to ice by ultrasonic vibration 2. Generation of ice slurries and effect of bubble nuclei, Int. J. Heat Mass Transf. 44 (23) (Dec. 2001) 4533–4539, https://doi.org/10.1016/S0017-9310(01)00058-8.
[18] T. Hozumi, A. Saito, S. Okawa, T. Matsui, Freezing phenomena of supercooled water under impacts of ultrasonic waves, Int. J. Refrig. 25 (7) (Nov. 2002) 948–953, https://doi.org/10.1016/S0140-7007(01)00104-9.
[19] X. Zhang, T. Inada, A. Tezuka, Ultrasonic-induced nucleation of ice in water containing air bubbles, Ultrason. Sonochem. 10 (2) (Mar. 2003) 71–76, https://doi.org/10.1016/S1350-4177(02)00151-7.
[20] R. Chow, R. Blindt, R. Chivers, M. Povey, A study on the primary and secondary nucleation of ice by power ultrasound, Ultrasonics 43 (4) (Feb. 2005) 227–230, https://doi.org/10.1016/j.ultras.2004.06.006.
[21] A. Olmo, R. Baena, R. Risco, Use of a droplet nucleation analyzer in the study of water freezing kinetics under the influence of ultrasound waves, Int. J. Refrig. 31 (2) (Mar. 2008) 262–269, https://doi.org/10.1016/j.ijrefrig.2007.05.012.
[22] L.S. Jia, W. Cui, Y. Chen, Y.A. Li, J. Li, Effect of ultrasonic power on super-cooling of TiO2 nanoparticle suspension, Int. J. Heat Mass Transf. 120 (May 2018) 909–913, https://doi.org/10.1016/j.ijheatmasstransfer.2017.12.128.
[23] W. Cui, L. Jia, Y. Chen, Y. Li, J. Li, S. Mo, Supercooling of Water Controlled by Nanoparticles and Ultrasound, Nanoscale Res. Lett. 13 (1) (Dec. 2018) 145, https://doi.org/10.1186/s11671-018-2560-z.
[24] Y. Liu, Y. Liu, P. Hu, X. Li, R. Gao, Q. Peng, L. Wei, The effects of graphene oxide nanosheets and ultrasonic oscillation on the supercooling and nucleation behavior of nanofluids PCMs, Microfluid. Nanofluidics 18 (1) (2015) 81–89, https://doi.org/10.1007/s10404-014-1411-1.
[25] N. Bhargava, R.S. Mor, K. Kumar, V.S. Sharanagat, Advances in application of ultrasound in food processing: A review, Ultrason. Sonochem. 70 (June 2020) (2021), https://doi.org/10.1016/j.ultsonch.2020.105293.
[26] Z. Zhu, P. Zhang, D.W. Sun, Effects of multi-frequency ultrasound on freezing rates and quality attributes of potatoes, Ultrason. Sonochem. 60 (June 2019) (2020) 104733, https://doi.org/10.1016/j.ultsonch.2019.104733.
[27] M. Singla, N. Sit, Application of ultrasound in combination with other technologies in food processing: A review, Ultrason. Sonochem. 73 (2021) 105506, https://doi.org/10.1016/j.ultsonch.2021.105506.
[28] X. Fu, T. Belwal, G. Cravotto, Z. Luo, Sono-physical and sono-chemical effects of ultrasound: Primary applications in extraction and freezing operations and influence on food components, Ultrason. Sonochem. 60 (2020) 104726, https://doi.org/10.1016/j.ultsonch.2019.104726.
[29] X. Cheng, M. Zhang, B. Xu, B. Adhikari, J. Sun, The principles of ultrasound and its application in freezing related processes of food materials: A review, Ultrason. Sonochem. 27 (Nov. 2015) 576–585, https://doi.org/10.1016/j.ultsonch.2015.04.015.
[30] L. Zheng, D.-W.-W. Sun, Innovative applications of power ultrasound during food freezing processes - A review, Trends Food Sci. Technol. 17 (1) (Jan. 2006) 16–23, https://doi.org/10.1016/j.tifs.2005.08.010.
[31] "Engineering and Operating Guide for DOWTHERM SR-1 and DOWTHERM 4000 Inhibited Ethylene Glycol-based Heat Transfer Fluids," DOWTHERM, 2008. [Online]. Available: https://www.dow.com/content/dam/dcc/documents/en-us/app-tech-guide/180/180-01190-01-engineering-and-operating-guide-for-dowtherm-sr1-and-dowtherm-4000.pdf?iframe=true.
[32] J.P. Holman, Experimental methods for engineers, 8th ed., McGraw-Hill/Connect Learn Succeed, Boston, 2012.
[33] Y.A. Çengel, A.J. Ghajar, *Heat and mass transfer: fundamentals \& applications*, Fifth ed., McGraw Hill Education, New York, NY, 2015.
[34] W. S. Rasband, "ImageJ." U. S. National Institutes of Health, Bethesda, Maryland, USA, [Online]. Available: https://imagej.nih.gov/ij/.
[35] R. Hickling, Nucleation of freezing by cavity collapse and its relation to cavitation damage, Nature 206 (4987) (1965) 915–917, https://doi.org/10.1038/206915a0.
[36] J.D. Hunt, K.A. Jackson, Nucleation of solid in an undercooled liquid by cavitation, J. Appl. Phys. 37 (1) (1966) 254–257, https://doi.org/10.1063/1.1707821.
[37] C.P. Lee, T.G. Wang, The effects of pressure on the nucleation rate of an undercooled liquid, J. Appl. Phys. 71 (11) (1992) 5721–5723, https://doi.org/10.1063/1.350510.
[38] A.J. Walton, G.T. Reynolds, Sonoluminescence, Adv. Phys. 33 (6) (Sep. 1984) 595–660, https://doi.org/10.1080/00018738400101711.
[39] L.A. Crum, Acoustic cavitation series: part five rectified diffusion, Ultrasonics 22 (5) (Sep. 1984) 215–223, https://doi.org/10.1016/0041-624X(84)90016-7.
[40] P. Gao, X. Zhou, B. Cheng, D. Zhang, G. Zhou, Study on heat and mass transfer of droplet cooling in ultrasound wave, Int. J. Heat Mass Transf. 107 (Sep. 2017) 916–924, https://doi.org/10.1016/j.ijheatmasstransfer.2016.11.002.
[41] A. Bamasag, H. Daghooghi-Mobarakeh, T. Alqahtani, P. Phelan, Performance enhancement of a submerged vacuum membrane distillation (S-VMD) system using low-power ultrasound, J. Memb. Sci. 621 (December 2020) (2021) 119004, https://doi.org/10.1016/j.memsci.2020.119004.
[42] Y.A. Çengel, M. Boles, Thermodynamics : An Engineering Approach, 8th ed., McGraw-Hill Higher Education, Boston, 2015.